Bubble Seeding Nanocavities: Multiple Polymer Foam Cell Nucleation by Polydimethylsiloxane-Grafted Designer Silica Nanoparticles

Shanqiu Liu,[†] Sida Yin,[†] Joost Duvigneau,[†] and G. Julius Vancso*,[†]*

[†]Materials Science and Technology of Polymers, MESA+ Institute for Nanotechnology, University of Twente, P.O. Box 217, 7500AE, Enschede, the Netherlands.

*Corresponding authors: j.duvigneau@utwente.nl (J. Duvigneau); g.j.vancso@utwente.nl (G. J. Vancso)

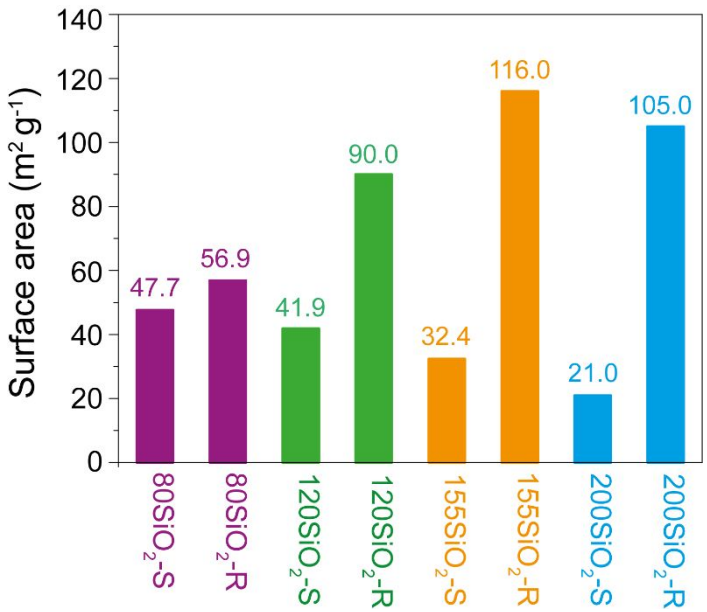

Figure S1. The specific surface area determined by BET measurements of SiO_2-S and SiO_2-R NPs with a diameter of ~ 80 nm, ~120 nm, ~155 nm and ~ 200 nm.

Brunauer-Emmet-Teller (BET) measurements were used to determine the surface area of the prepared silica NPs. The results are shown in Figure S1. It is obvious that the surface area of NPs was significantly increased after $NaBH_4$ treatment. For the NPs with a diameter of 155 nm the surface area increased from 32.4 $m^2 g^{-1}$ ($155SiO_2$-S) to 116.0 $m^2 g^{-1}$ ($155SiO_2$-R). Nearly 3.6-fold increase in surface area is in good agreement with the 3.4 times higher grafted amount of PDMS to these particles.

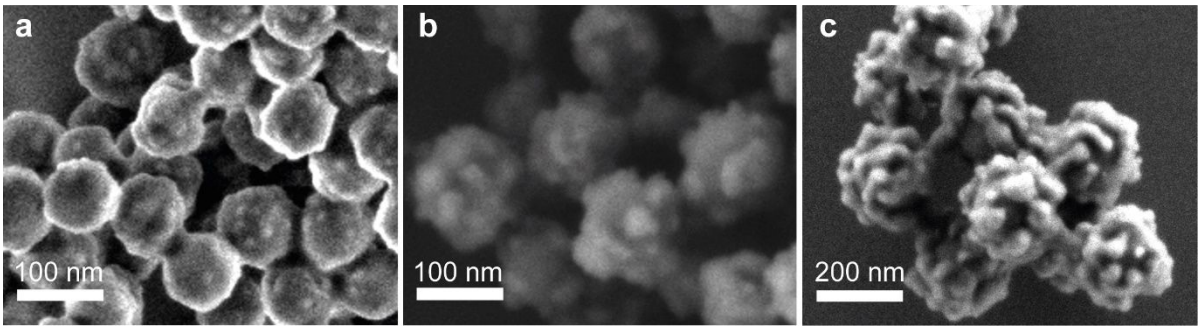

Figure S2. SEM images showing SiO_2-R NPs with a diameter of (a) ~ 80 nm, (b) ~ 120 nm, and (c) ~ 200 nm.

Figure S2 shows the SEM images of the SiO_2-R NPs with diameters of ~ 80 nm, ~ 120 nm and ~ 200 nm. Figure S3 shows cross sectional SEM images of the 80 nm series of particles melt blended in PMMA as a repsresentative case to demonstrate the particle disperion in the composite. From Figure S3 it is clear that a good particle dispersion was obtained by melt blending.

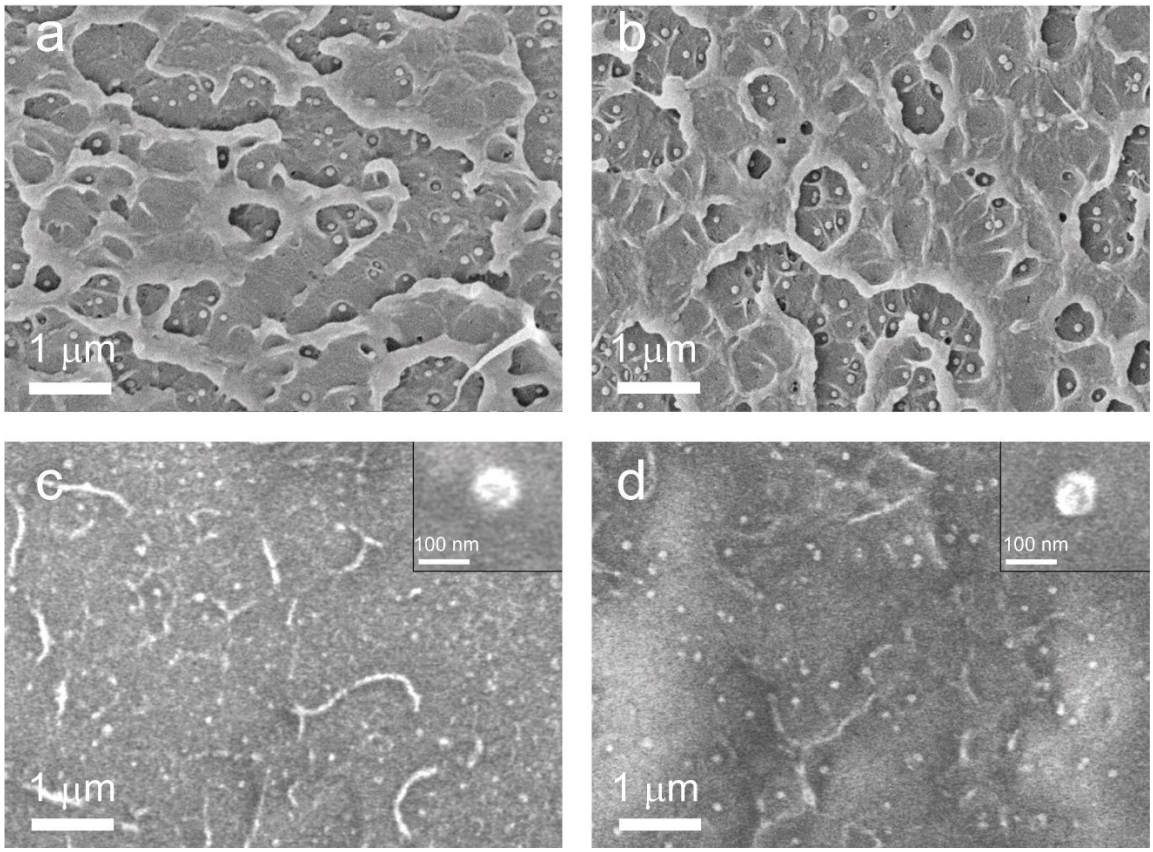

Figure S3. Cross-sectional SEM images showing the dispersion of (a) 80SiO_2-S, (b) 80SiO_2-SP, (c) 80SiO_2-R and (d) 80SiO_2-RP in PMMA.

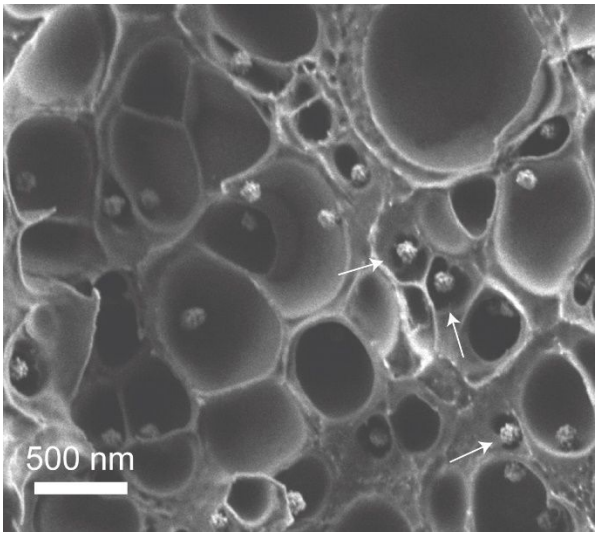

Figure S4. SEM images of cross-sectioned PMMA foams nucleated by 120SiO_2-RP. The saturation pressure, foaming temperature and foaming time were 55 bar, 40 °C and 1 second, respectively. The white arrows point towards the particles showing multiple cell nucleation events per particle.

Figure S4 shows the SEM images of cross-sectioned PMMA foams nucleated by 120SiO_2-RP. The multiple cells nucleation events were observed for some of the particles.

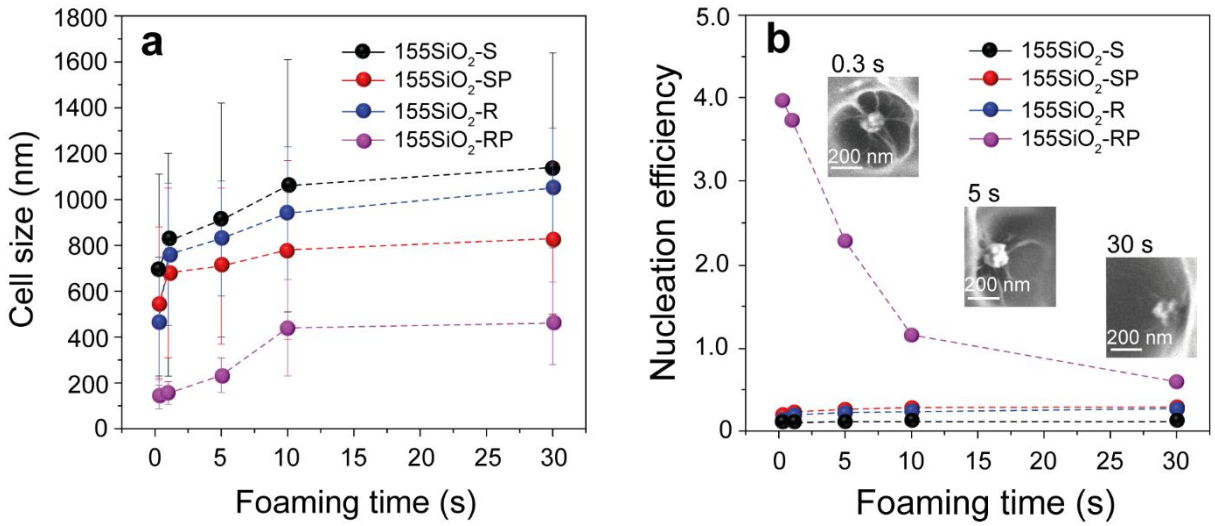

Figure S5. (a) Foam cell size and (b) cell nucleation efficiency as a function of foaming time for PMMA foams nucleated by 155SiO_2-S, 155SiO_2-SP, 155SiO_2-R and 155SiO_2-RP NPs. The used saturation pressure and foaming temperature were 55 bar and 40 °C, respectively.

The cell size and cell nucleation efficiency for PMMA foams nucleated by 155SiO_2-S, 155SiO_2-SP, 155SiO_2-R and 155SiO_2-RP NPs were determined as a function of the foaming time. The results are shown in Figure S5. It is obvious that regardless of the type of NP used cell size of the corresponding PMMA foams increases as a function of foaming time up to 10 seconds after which it reaches a plateau value with a size value that depends on the nucleating particle type used.

The cell nucleation efficiency of PMMA foams containing 155SiO_2-SP is higher compared to those containing 155SiO_2-S for the same foaming time (as shown in Figure S5b), which is ascribed to the high CO_2-philicity and low surface energy of the thin PDMS shell of the 155SiO_2-SP NPs.[1] Interestingly, the raspberry-like NPs, *i.e.,* 155SiO_2-R, show a higher cell nucleation efficiency compared to that of 155SiO_2-S, as well. This is ascribed to the presence of cavities on the raspberry-like nanoparticle surfaces, resulting in energetically favorable cell nucleation.[2] The nucleation efficiency of PMMA foams nucleated by 155SiO_2-RP decreases upon increasing the foaming time. This is due to the observed cell coalescence occurring during the early stages of foaming (see Figure 5c-f). Notably, the nucleation efficiency of 155SiO_2-RP is well above 1 within the first 10 seconds of foaming, which is ascribed to the multiple cell nucleation events occurring per nucleating 155SiO_2-RP particle. The excellent nucleation performance of 155SiO_2-RP is ascribed to the energetically favorable cell nucleation from the particles surface cavities combined with the presence of a CO_2 philic PDMS layer around the 155SiO_2-RP NPs.[1, 3, 4]

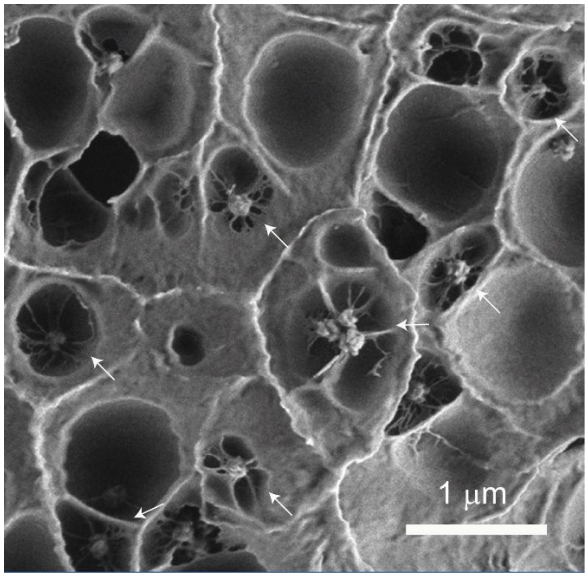

Figure S6. SEM images of cross-sectioned polystyrene foams nucleated by 150SiO_2-RP. The saturation pressure, foaming temperature and foaming time were 55 bar, 100 °C and 1 second, respectively. The white arrows point towards the particles showing multiple cell nucleation events per particle.

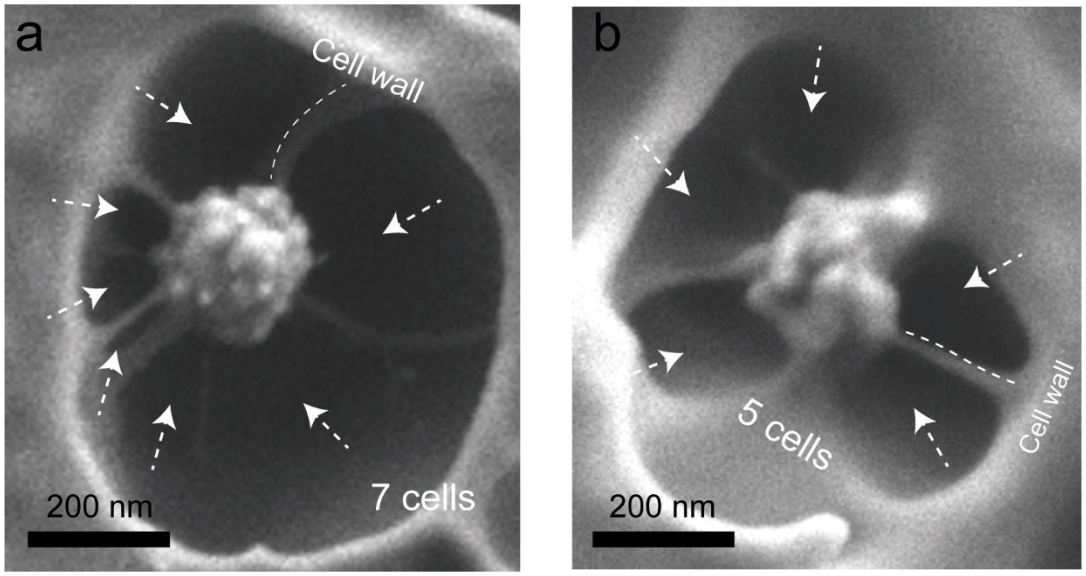

Figure S7. SEM image showing multiple nucleating events at individual 200 SiO_2-RP particles. The white arrows point at the cells we included in the calculation of the cell density. We counted cells only when the cell walls were clearly visible.

REFERENCES

(1) Liu, S.; Eijkelenkamp, R.; Duvigneau, J.; Vancso, G. J. Silica-Assisted Nucleation of Polymer Foam Cells with Nanoscopic Dimensions: Impact of Particle Size, Line Tension, and Surface Functionality. *ACS Appl. Mater. Interfaces* **2017,** *9*, 37929–37940.

(2) Liu, Q.; Zhu, Y.; Yang, G.; Yang, Q. Nucleation Thermodynamics inside Micro/Nanocavity. *J. Mater. Sci. Technol.* **2008,** *24*, 183–186.

(3) Qian, M.; Ma, J. The Characteristics of Heterogeneous Nucleation on Concave Surfaces and Implications for Directed Nucleation or Surface Activity by Surface Nanopatterning. *J. Cryst. Growth* **2012,** *355*, 73–77.

(4) Maksimov, A. O.; Kaverin, A. M.; Baidakov, V. G. Heterogeneous Vapor Bubble Nucleation on a Rough Surface. *Langmuir* **2013,** *29*, 3924–3934.